



Potential of thin-film silicon solar cells by using high haze TCO superstrates

J. Krc^a, B. Lipovsek^a, M. Bokalic^a, A. Campa^a, T. Oyama^b, M. Kambe^b, T. Matsui^c, H. Sai^c,
M. Kondo^c, M. Topic^{a,*}

^a University of Ljubljana, Faculty of Electrical Engineering, Trzaska 25, 1000 Ljubljana, Slovenia

^b Asahi Glass Co. Ltd. Research Center, 1150 Hazawa-cho, Kanagawa-ku, Yokohama, Kanagawa 221-8755, Japan

^c National Institute of Advanced Industrial Science and Technology (AIST) Research Center for Photovoltaics, Central 2, Umezono 1-1-1 Tsukuba 305-8868, Japan

ARTICLE INFO

Available online 13 October 2009

Keywords:

Thin-film silicon solar cell
Double textured TCO
Optical modelling

ABSTRACT

Potential improvements in the performance of tandem amorphous silicon/microcrystalline silicon (a-Si:H/ μ -Si:H) solar cells, related to the TCO superstrates with enhanced scattering properties are studied. In particular, optical effects of a high haze double textured (W-textured) SnO₂:F TCO superstrate are analyzed and compared to the properties of the pyramidal type SnO₂:F TCO superstrate. Solar cell with W-textured superstrate exhibits higher long-wavelength external quantum efficiency of the bottom μ -Si:H cell than the one with pyramidal type TCO superstrate. Optical simulations are employed to study the potential improvements of the solar cell performance if ideal haze parameter ($H=1$) and/or a broad angular distribution function (Lambertian) of scattered light are applied to textured interfaces in the solar cell structure. Simulations reveal significant improvements in long-wavelength quantum efficiencies if a broad angular distribution function of scattered light is applied. Optical losses in the cells with enhanced scattering properties are analysed and evaluated in terms of short-circuit current losses in the supporting layers and losses due to reflected light.

© 2009 Elsevier B.V. All rights reserved.

1. Introduction

Thin-film silicon (Si) technology has gained an important position in photovoltaic industry and market. Small material consumption, low-temperature deposition processes applicable to large areas in either batch or roll-to-roll production lines make thin-film Si solar cells and modules competitive to other solar cells, regarding total costs and state-of-the-art performances [1]. In order to boost the conversion efficiency of the thin-film silicon solar cells and/or to reduce the thickness of absorber layers further (meaning shorter deposition times, smaller material consumption), advanced light trapping techniques are of great importance [2]. They are aiming to efficiently scatter the light in the cell, in order to increase the absorption in the active layers (absorbers), whereas optical losses in the supporting layers (contacts, doped layers) and reflectance from the cell should be minimized. Textured transparent conductive oxide (TCO) superstrates are used to introduce surface texture and light scattering within the solar cell structures in so-called superstrate configuration (light entering through the transparent superstrate). Typically, SnO₂:F [3], magnetron sputtered ZnO:Al [4] or LPCVD ZnO:B [5] TCOs deposited on glass carrier are used as superstrates for thin-film Si solar cells. The textures of the TCO surfaces are pyramidal (SnO₂:F, ZnO:B) or crater-like (ZnO:Al after etching). Recently, novel

types of high haze SnO₂:F TCO superstrates with double-texture (W-texture) surface morphology have been developed [6]. These TCO superstrates are aiming to significantly boost the scattering level (haze), especially at longer wavelengths ($\lambda > 600$ nm), to enhance the long-wavelength absorption in microcrystalline Si (μ -Si:H) based single junction or tandem amorphous Si/microcrystalline Si (a-Si:H/ μ -Si:H) solar cells. Similar transparency of W-textured TCOs can be achieved as in the case of pyramidal type of surface texture. [7].

In this work we focus on experimental and theoretical study of TCOs with enhanced scattering properties and investigate their role on the performance of a tandem a-Si:H/ μ -Si:H solar cell. In particular, optical effects of high haze W-textured TCO superstrates are studied. After showing the advantages of W-textured TCO superstrates over SnO₂:F TCO superstrates with pyramidal like surface texture optical simulations are employed to investigate the role of further improvements in scattering properties of TCO superstrates. Beside high haze the importance of a broad angular distribution function of scattered light of the TCO superstrates is revealed. Further on, optical losses in the supporting layers are studied. The losses in the back reflector are indicated as one of the limiting factors for further improvements.

2. Simulation method

A one-dimensional semi-coherent optical simulator SunShine was used for theoretical investigations [8]. In the simulator, direct (non-scattered) light is analyzed in terms of coherent electromagnetic

* Corresponding author. Tel.: +386 1 4768 470; fax: +386 1 4264 630.
E-mail address: janez.krc@fe.uni-lj.si (M. Topic).

waves, whereas for scattered light ray tracing is applied. Reflection, transmission and light scattering properties of each textured interface are taken into account for incoming waves and rays in simulations. Main input parameters of the simulator are: thicknesses of layers, including thick glass at the front, wavelength-dependent complex refractive indices of individual layers, light scattering parameters of textured interfaces, calibration functions for total reflectance at (textured) interfaces and solar illumination spectrum. The scattering parameters are: haze, H , which describes the scattering level of reflected and transmitted light and the angular distribution function, ADF , which describes directional dependency of scattered light. The H and the ADF parameters for reflected and for transmitted light can be calibrated with the measured scattering properties for specific TCO superstrate [9]. Modified equations of scalar scattering theory are used in the simulator to transfer the measured H , (typically determined for the TCO superstrate in air surrounding) to internal interfaces in the solar cell structures [10–12]. Accurate transformation of the ADF from external measurements in air to internal interfaces is more critical and requires either extensive simulation fitting procedures (based on the analysis of partial solar cell structures) or two- and three-dimensional modelling that considers accurate surface morphology of the textured interface. In a first order approximation the ADF measured externally (e.g. at TCO/air interface) is directly applied to internal interfaces in the solar cell structure.

Main results obtained from the optical simulations with the SunShine are the wavelength-dependent light reflectance from the structure, the absorptance in each layer (absorbed light in active layers, optical losses in supporting layers) and the optical generation rate profile. Considering an ideal extraction of the generated charge carriers in the absorber layers and neglecting the contributions from the doped layers, the calculated absorptance of the absorber layers can be considered as the external quantum efficiency of the solar cells. In this way also short-circuit current density can be determined from the absorptance for the solar spectrum used (AM1.5).

3. Results and discussion

Optical effects of the two types of textured TCO superstrates were investigated: a pyramidal type (known as Asahi U type) and high haze W-textured $\text{SnO}_2:\text{F}$ TCO superstrate. Their haze parameters for transmitted light and Scanning Electron Microscope (SEM) pictures of the textured TCO surface morphology are shown in Figs. 1 and 2, respectively. Whereas in the case of pyramidal type TCO randomly

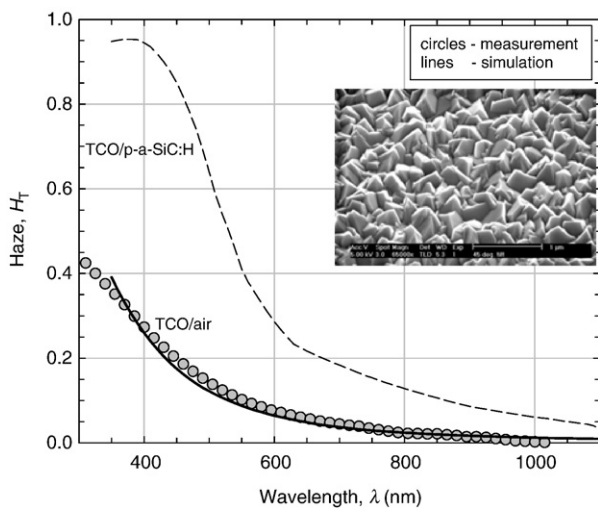


Fig. 1. Haze parameter of the pyramidal type TCO (Asahi U) superstrate measured in air (simulation and measurement) and for TCO/p-a-SiC:H interface (simulation). Scanning Electron Microscopy picture of the TCO surface is shown in the inset.

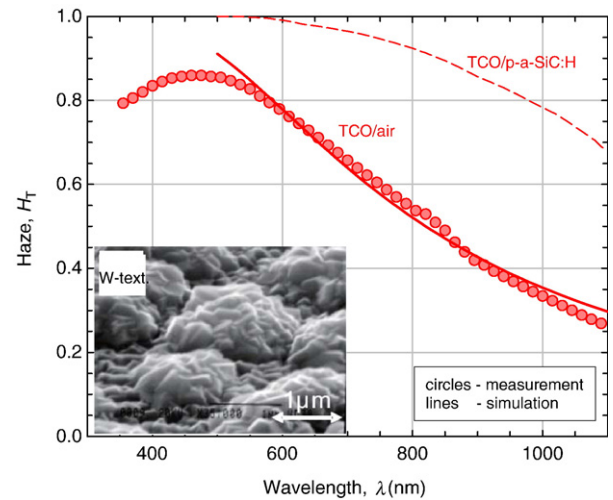


Fig. 2. Haze parameter of the W-textured TCO measured in air (measurement and simulation) and for TCO/p-a-SiC:H interface (simulation). Scanning Electron Microscopy picture of the TCO surface is shown in the inset.

distributed pyramid-grains are present at the surface, in the case of W-textured TCO two types of texturing features are superimposed: small pyramids on top of larger hemi-spheres. Details about the electrical properties and the deposition methods of the TCOs can be found elsewhere [3,7], here we focus our investigation on light scattering properties only. Measurements in the air are presented by circles in the figures. Illumination was applied from the glass side of the samples. Lines present the simulations in which equations of scalar scattering theory were used to approximate the wavelength-dependent haze behavior [10,11]. Significantly higher haze in short- and especially long-wavelength region is observed for the W-textured TCO, compared to the pyramidal type TCO superstrate. A shallow peak in the measured H at $\lambda \approx 500$ nm is observed for the selected W-textured TCO due to the presence of two types of texturing. In simulations the equations of scalar scattering theory were calibrated on haze measurements at the TCO/air interface and were then used to determine the haze parameter at internal interfaces (e.g. for TCO/p-a-SiC:H as shown in the graphs and other interfaces) in a solar cell structure [12]. Simulations revealed that simulated haze at TCO/p-a-SiC:H interface has significantly higher values than the one determined at TCO/air interface. Following the scalar scattering theory higher difference in the refractive indexes between the incident medium (TCO) and the medium in transmission (p-a-SiC:H) leads to a higher scattering level for the transmitted light [11]. Thus, at internal interfaces formed by layers with high difference in the refractive indexes (like TCO with $n \approx 1.9$ and p-a-SiC:H with $n \approx 3.3$ at $\lambda = 600$ nm), much higher haze is expected than the one determined in air surrounding, for both types of TCO superstrates.

Tandem a-Si:H/ $\mu\text{c-Si:H}$ solar cells were deposited by PECVD on both types of TCO superstrates. The thicknesses of the top i-a-Si:H and the bottom $\mu\text{-c-Si:H}$ absorber layer were $0.35 \mu\text{m}$ and $1.5 \mu\text{m}$, respectively. For the back reflector ZnO/Ag was used. No intermediate reflector was applied between the top and the bottom cell. The results of the measured external quantum efficiency, QE , are shown in Fig. 3 (symbols). Almost no changes are observed in the quantum efficiencies corresponding to the top cell, QE_{top} , when using pyramidal type or W-textured TCO superstrate. However, in the quantum efficiency of the bottom cell, QE_{bot} , noticeable increase in the long-wavelength region can be observed for the W-textured superstrate (due to enhanced long-wavelength scattering). The corresponding J_{SC} values of the top cell are $J_{\text{SC top}} \approx 11.8 \text{ mA/cm}^2$ for cells on both types of TCO superstrates and $J_{\text{SC bot}} \approx 10.4 \text{ mA/cm}^2$ and 11.9 mA/cm^2 for the cell on pyramidal and the W-textured TCO superstrates,

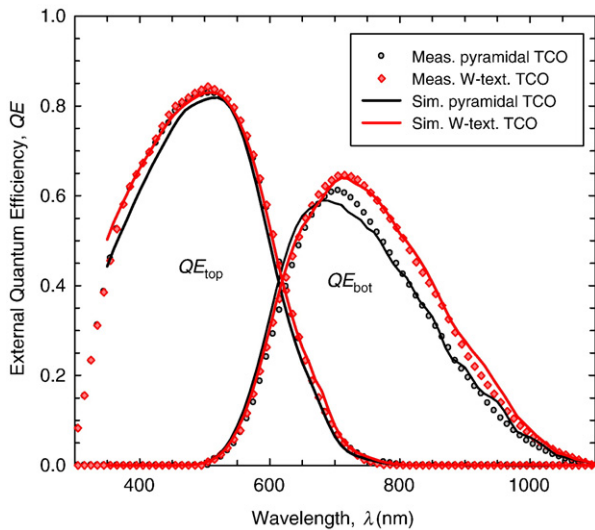


Fig. 3. Measured and simulated external quantum efficiencies of the top and the bottom cell in a-Si:H/ μ c-Si:H tandem configuration ($d_{\text{top}} = 0.35 \mu\text{m}$, $d_{\text{bot}} = 1.5 \mu\text{m}$) deposited on the pyramidal type and W-textured TCO superstrate.

respectively. This means that the W-textured TCO superstrate leads to around 12% increase in $J_{\text{SC bot}}$.

For the analysis of optical situation in the solar cell structures we employed our optical simulator SunShine, which we calibrate with the optical parameters of the layers (complex refractive indexes, layer thicknesses) and scattering parameters of the interfaces (H and ADF) for the cells on the two TCO superstrates. The ADF measurements of the W-textured TCO are presented in Fig. 4. The ADF that corresponds to longer wavelengths ($\lambda = 960 \text{ nm}$) has a broader shape, which means more scattering into larger angles, than in case of shorter wavelengths ($\lambda = 633 \text{ nm}$). The comparison of the ADF of W-textured TCO with pyramidal type TCO (not shown here) reveals somewhat narrower ADF of the W-textured TCO in short-wavelength region ($\lambda < 650 \text{ nm}$), however, for longer wavelengths the ADF of the W-textured TCO is broadened, which improves the scattering and thus long-wavelength absorption in μ c-Si:H.

Assuming good extraction of generated charge carriers in absorber layers (i-a-Si:H and i- μ c-Si:H) and neglecting the small contribution from the p- and n-doped layers, simulated absorptances in the top and the bottom absorber are directly compared with the measured QEs of

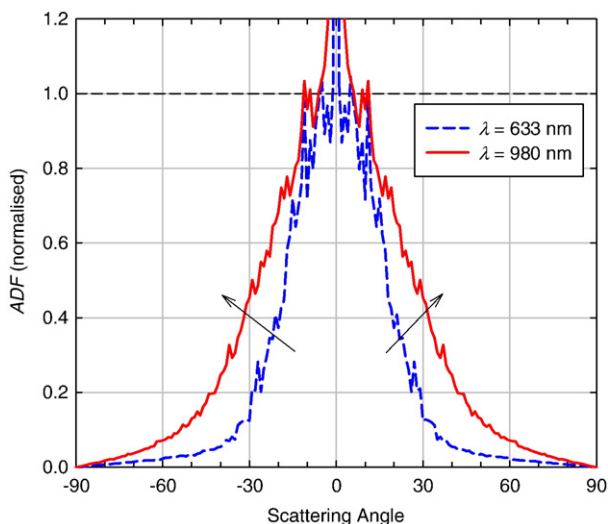


Fig. 4. Measured angular distribution function of transmitted light (measured in a plane perpendicular to the sample) of W-textured TCO superstrate.

the analyzed solar cell. Using the calibrated optical simulator the simulated absorptances in the top and the bottom absorber (full lines in Fig. 3) are in good agreement with the measured QE_{top} and QE_{bot} , for both solar cells with different TCO superstrates. The same trend of increased long-wavelength QE_{bot} as observed in measurements is obtained also in simulations. Based on the agreement with the experimental data, simulations were then used further to analyze the optical situation in the cells with W-textured TCO superstrate and to examine the potential of possible further improvements in solar cell performance, related to enhanced light scattering properties.

First, potential thickness reductions of the bottom i- μ c-Si:H absorber layer, d_{bot} , related to the use of the W-textured TCO superstrate are indicated by means of optical simulations. In Fig. 5 the $J_{\text{SC bot}}$ is shown as a function of d_{bot} for the solar cells with both types of TCO superstrates. Linear dependency between $J_{\text{SC bot}}$ and d_{bot} is observed in the semi-logarithmic plot. From the plot, one can see, for example, that 20% thinner i- μ c-Si:H absorber ($1.2 \mu\text{m}$) can be used in the case of W-textured TCO superstrate than in the case of pyramidal type TCO superstrate (reference $d_{\text{bot}} = 1.5 \mu\text{m}$), to achieve the same level of $J_{\text{SC bot}}$. Further on, about 30% thicker i- μ c-Si:H absorber ($1.95 \mu\text{m}$) should be used in the cell with pyramidal type of TCO superstrate to achieve the same $J_{\text{SC bot}}$ as achieved in the cell with the W-textured superstrate ($d_{\text{bot}} = 1.5 \mu\text{m}$). These results indicate the possibilities for noticeable thickness reductions (and thus shortening the deposition times) of the i- μ c-Si:H absorber layer in the case of the use of high haze W-textured TCO superstrates.

Simulations were then further employed to analyze the optical losses in the a-Si:H/ μ c-Si:H solar cell with different TCO superstrates. Results of absorptances in the layers are presented in Fig. 6 for the solar cell with W-textured TCO superstrate. White area represents the share of light that is absorbed in the top and the bottom absorber and that is utilized for the photocurrent generation. The colored areas are the absorptances in p- and n-doped layers (p + n), in glass/SnO₂:F W-textured TCO superstrate, (TCO superstrate), in back reflector, BR, (ZnO/Ag) and optical losses due to reflected light from the cell (R). One can observe that in the short-wavelength region the optical losses in p + n layers predominate (primarily losses in the p-a-Si:H layer of the top cell), whereas at longer wavelengths losses in TCO superstrate and back reflector, besides the losses due to reflected light, start to play a role. Also it is important to evaluate the losses in terms of J_{SC} due to light absorption in non-active layers. The relative shares of J_{SC} losses are presented in Fig. 7 (solar spectrum utilization). From this

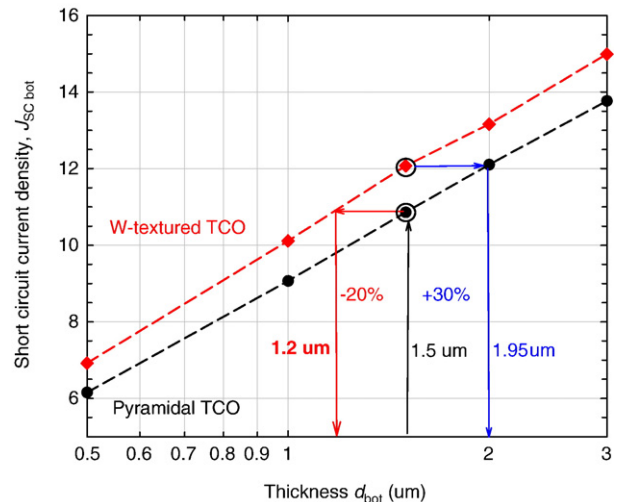


Fig. 5. Simulated short-circuit current density of bottom μ c-Si:H cell as a function of the i- μ c-Si:H absorber thickness, d_{bot} , for the pyramidal type (bottom dashed line) and W-textured TCO superstrates (top dashed line). Two open circles denote the measured values for the thickness $d_{\text{bot}} = 1.5 \mu\text{m}$, whereas the closed circles are simulation points. The lines are guides for the eye.

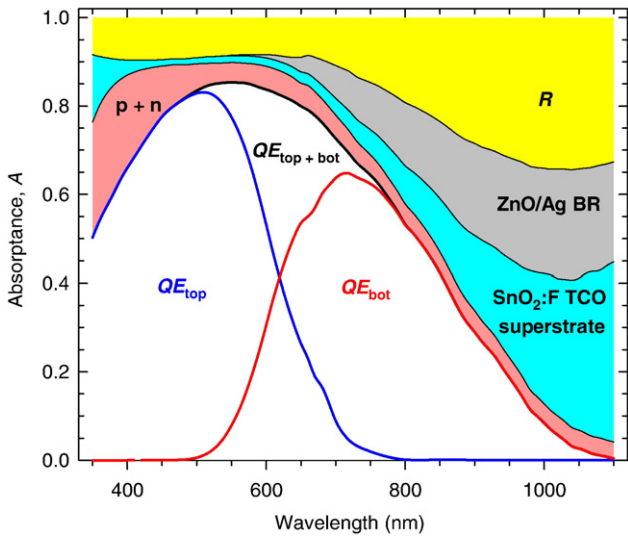


Fig. 6. Optical loss diagram for a-Si:H/μc-Si:H solar cell with W-textured TCO superstrate.

graph one can observe that in the solar cell with W-textured TCO (second bar-line from the top) about 27.4% (11.79 mA/cm²) and 28.1% (12.07 mA/cm²) of theoretically available J_{SC} (AM 1.5 spectrum, $\lambda = 350 - 1100$ nm) is utilized in the top and the bottom absorber, respectively. The 17.6% share (7.54 mA/cm²) is lost due to reflected (non-absorbed) light. Among the supporting layers one should mention 10.6% share (4.56 mA/cm²) in the TCO superstrate and 10.2% (4.40 mA/cm²) in the back reflector. Comparing optical losses of the cell with the W-textured TCO superstrate to the one with the pyramidal type TCO superstrate (top bar-line) one can observe a decrease in optical losses for the W-textured TCO related to reflected light (from 26.3% to 17.7%). This is because better light trapping is employed in the cell with the W-textured TCO. However, the J_{SC} improvements in the bottom absorber are from 25.4% to 28.1%, at the same time enhanced optical losses in back reflector are detected.

At this stage we focus our investigation to further reductions of optical losses originating from reflected light, which can be done by improving scattering properties (parameters) of the TCO superstrate. For this reason in simulations we (a) boost the haze parameter of all textured interfaces to the ideal value $H=1$ (b) broaden the ADF to Lambertian (cosine) distribution function and (c) use the combination of both, $H=1$ and Lambertian ADF. Mentioned scattering parameters were applied to the TCO superstrate and consequently to all other textured interfaces (from TCO/p-a-SiC:H on) in the

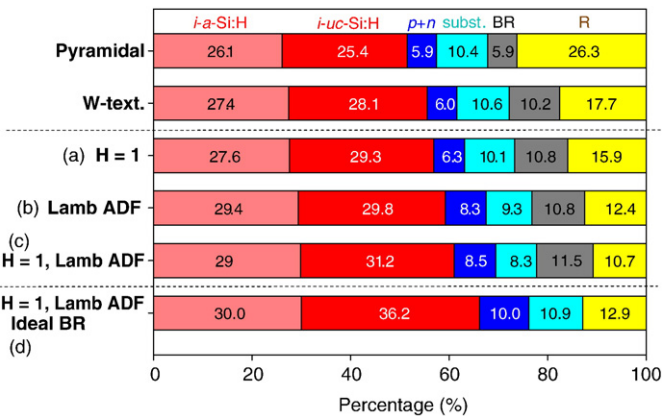


Fig. 7. Solar spectrum utilization – short-circuit current distribution (in %) in active layers (i-a-Si:H and i-μc-Si:H), J_{SC} losses in supporting layers and losses due to reflected light. The active layer thicknesses are $d_{top} = 0.35 \mu\text{m}$ and $d_{bot} = 1.5 \mu\text{m}$.

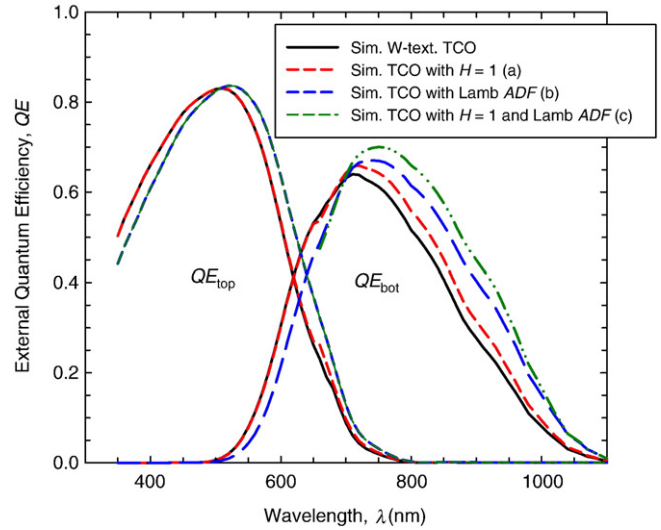


Fig. 8. Improvements in external quantum efficiencies of the top a-Si:H and the bottom μc-Si:H solar cell related to the ideal haze ($H=1$) and broad angular distribution function of scattered light (Lambertian ADF).

analyzed solar cell structure. All other optical parameters were kept the same as in the case of simulation of the solar cell with W-textured TCO superstrate. The results of QEs in cases (a)–(c) are presented in Fig. 8. For comparison QEs of the solar cell with W-textured TCO superstrate (scattering parameters of W-textured TCO) are shown. In the case of (a), $H=1$, one can observe further increase in long-wavelength QE_{bot} , while QE_{top} remains mostly unchanged. In the case of (b), Lambertian ADF, noticeable increase in both, the long-wavelength QE_{top} and especially in the long-wavelength QE_{bot} is observed. In the case of (c), combination of $H=1$, and Lambertian ADF, further improvements in the long-wavelength QE_{bot} are indicated.

These results show that besides enhancing haze parameter of the TCO superstrates (and consequently of internal interfaces) special

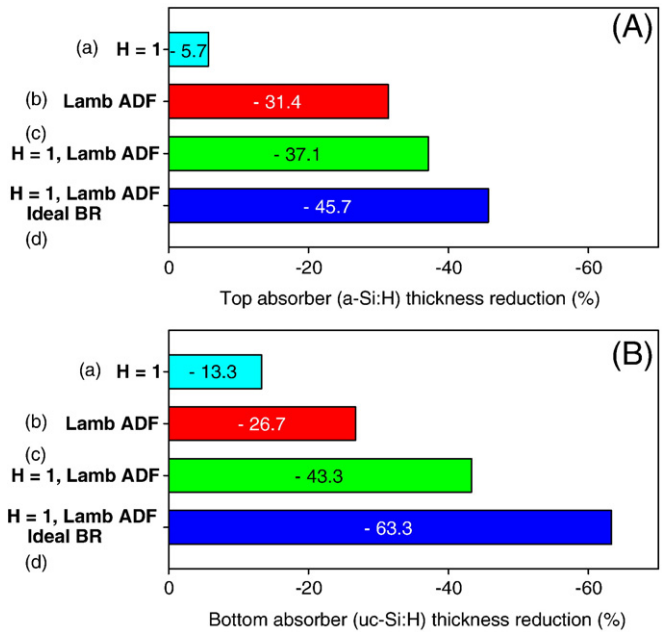


Fig. 9. Potential thickness reductions of (A) top i-a-Si:H and (B) bottom i-μc-Si:H absorber related to improved scattering parameters of textured TCO superstrate. As the reference the solar cell with W-textured TCO superstrate ($d_{top} = 0.35 \mu\text{m}$ and $d_{bot} = 1.5 \mu\text{m}$) was taken.

attention has to be paid to develop the textured morphologies of the TCO superstrates that would enable a broad *ADF* of the scattered light.

The J_{SC} distribution in the top (i-a-Si:H) and the bottom absorber ($\mu\text{-Si:H}$) and J_{SC} losses in the supporting layers and due to reflected light in cases (a)–(c) can be found in Fig. 7. Compared to the solar cell with W-textured TCO superstrate the losses due to reflected light are in the case of (c) significantly reduced from 17.7% to 10.7%. The corresponding J_{SC} shares related to the top and the bottom absorber are increased from 27.4% to 28.9% for the top cell and from 28.1% to 31.2% for the bottom cell, the rest is lost due to increased absorptances in non-active layers. Thus, further improvements in the cell can be done only by minimizing the optical losses in the supporting layers, especially in the back contact/reflector (11.5% share of J_{SC} was lost therein in the case of (c)). Simulation results show that by applying an ideal back reflector (such as optimized dielectric back reflector with negligible absorption, case (d)) in the solar cell with enhanced scattering properties the share of $J_{SC\ top}$ and $J_{SC\ bot}$ would be almost unchanged for top cell (30%) and significantly improved for the bottom cell (36.6%). However, at the same time the J_{SC} losses are increased in TCO superstrate, p- and n-doped layers and due to reflected light as a consequence of ideal reflectance at the back side of the solar cell. It has to be mentioned that the share of J_{SC} in the top and the bottom absorber layer could be larger, if thicker absorbers are applied. However, the tendency is to use thin absorber layers. Therefore, we rather focus on potential thickness reductions that can be achieved with TCO superstrates with enhanced scattering parameters, maintaining the J_{SC} of the top and the bottom cell unchanged. The results of thickness reductions of the top and the bottom absorber in cases (a)–(d) are shown in Fig. 9. As the reference, the solar cell with W-textured TCO superstrate, with $d_{i\ top} = 0.35\ \mu\text{m}$ and $d_{i\ bot} = 1.5\ \mu\text{m}$ was taken. Significant thickness reductions are indicated, especially for the bottom $\mu\text{-Si:H}$ absorber: –13.3% in the case of (a), –63.3% in the case of (d). The corresponding reduction of the top a-Si:H absorber is from –5.7% to –45.7% and is mostly a consequence of the broad *ADF*.

4. Conclusions

Effects of light scattering were analysed for a-Si:H/ $\mu\text{-Si:H}$ solar cell for two types of $\text{SnO}_2\text{:F}$ based TCO superstrates: with pyramidal

texture and W-textured TCO superstrate. An increase in the long-wavelength *QE* of the bottom cell was observed for W-textured TCO compared to the pyramidal type of TCO superstrate. Results of optical simulations indicate 20% of thickness reduction of the bottom absorber thickness (reference $d_{bot} = 1.5\ \mu\text{m}$) if the W-textured TCO is used instead of pyramidal type TCO superstrate. Further potential improvements in solar cell performances were studied by introducing ideal haze parameter, $H = 1$, and a broad *ADF* (Lambertian) in simulations. The results revealed further improvements, especially due to the broad *ADF*, where both, the long-wavelength QE_{top} and the long-wavelength QE_{bot} are enhanced, as a consequence of improved light trapping in the solar cell. The analysis of the optical losses for the cell with enhanced scattering properties reveals noticeable absorption losses in the back reflector (ZnO/Ag). Considering enhanced scattering parameters ($H = 1$, Lambertian *ADF*) and applying a back reflector without optical losses, simulation indicates that in this case the share of potentially available J_{SC} from AM 1.5 spectrum ($\lambda = 350\text{--}1100\ \text{nm}$) is 30% in the top absorber ($d_{top} = 0.35\ \mu\text{m}$) and 36.2% in the bottom absorber ($d_{bot} = 1.5\ \mu\text{m}$). By keeping the J_{SC} unchanged, the theoretical thickness reductions of the top and the bottom absorber are in this case –45.7% and –63.3%, respectively.

References

- [1] A. Jäger-Waldau, PV Status Report 2007, JRC Technical Notes, EUR 23018 EN, 2007.
- [2] A. Shah, et al., J. Non-Cryst. Solids 338–340 (2004) 639.
- [3] K. Sato, Y. Gotoh, Y. Hayashi, K. Adachi, H. Naishimura, Reports Res. Lab. Asahi Glass Co., Ltd, vol. 40, 1990, p. 233.
- [4] O. Kluth, G. Schöpe, B.J. Hüpkens, C. Agashe, J. Müller, B. Rech, Thin Solid Films 351 (1999) 247.
- [5] S. Fay, S. Dubail, U. Kroll, J. Meier, Y. Ziegler, A. Shah, Proc. 16th EU PVSEC, Glasgow, 2000, p. 361.
- [6] M. Kambe, K. Masumo, N. Taneda, T. Oyama, K. Sato, Tech. Dig. of the Intern PVSEC-17, Fukuoka, Japan, 2007, p. 1161.
- [7] T. Oyama, M. Kambe, N. Taneda, K. Masumo, Mat. Res. Soc. Proc. 1101 (2008) KK02.
- [8] J. Krc, F. Smole, M. Topic, Prog. Photovot. Res. Appl. 11 (2003) 15.
- [9] J. Krc, M. Zeman, O. Kluth, F. Smole, M. Topic, Thin Solid Films 426 (1–2) (2003) 296.
- [10] P. Beckmann, A. Spizzichino, The Scattering of Electromagnetic Waves from Rough Surfaces, Pergamon press, 1963.
- [11] K. Carniglia, Opt. Eng. 18 (2) (1979) 104.
- [12] J. Krc, M. Zeman, F. Smole, M. Topic, J. Appl. Phys. 92 (2) (2002) 749.